EUROPEAN ORGANIZATION FOR NUCLEAR RESEARCH

CERN-PPE/94-129
July 28, 1994

Updated measurement of the τ lifetime

The OPAL Collaboration

Abstract

We present an update of our measurement of the τ lepton lifetime, using data taken during 1992 and 1993 with the OPAL detector at LEP. The lifetime is determined from analyses of the impact parameters of tracks from τ decays to a single charged particle, and the reconstructed decay lengths from τ decays to three charged particles. With the added statistics (which increase the τ pair event sample size by more than a factor of four over our 1990 and 1991 data sample), the updated lifetime measurement is:

$$\tau_\tau \;=\; 288.8 \;\pm\; 2.2\;(\text{stat}) \;\pm\; 1.4\;(\text{sys})\;\text{fs}.$$

When combined with world-average measurements of the tau leptonic branching fractions (assuming e-μ universality), the ratio of charged-current couplings is:

$$\left(\frac{g_\tau}{g_\mu}\right) \;=\; 1.005 \;\pm\; 0.007\;,$$

in agreement with the hypothesis of τ-μ charged-current universality.

TO BE SUBMITTED TO PHYSICS LETTERS

The OPAL Collaboration

R. Akers[16], G. Alexander[23], J. Allison[16], K.J. Anderson[9], S. Arcelli[2], S. Asai[24], A. Astbury[28], D. Axen[29], G. Azuelos[18,a], A.H. Ball[17], E. Barberio[26], R.J. Barlow[16], R. Bartoldus[3], J.R. Batley[5], G. Beaudoin[18], A. Beck[23], G.A. Beck[13], J. Becker[10], C. Beeston[16], T. Behnke[27], K.W. Bell[20], G. Bella[23], P. Bentkowski[18], S. Bentvelsen[8], P. Berlich[10], S. Bethke[32], O. Biebel[32], I.J. Bloodworth[1], P. Bock[11], H.M. Bosch[11], M. Boutemeur[18], S. Braibant[12], P. Bright-Thomas[25], R.M. Brown[20], A. Buijs[8], H.J. Burckhart[8], C. Burgard[27], P. Capiluppi[2], R.K. Carnegie[6], A.A. Carter[13], J.R. Carter[5], C.Y. Chang[17], C. Charlesworth[6], D.G. Charlton[8], S.L. Chu[4], P.E.L. Clarke[15], J.C. Clayton[1], S.G. Clowes[16], I. Cohen[23], J.E. Conboy[15], M. Coupland[14], M. Cuffiani[2], S. Dado[22], C. Dallapiccola[17], G.M. Dallavalle[2], C. Darling[31], S. De Jong[13], H. Deng[17], M. Dittmar[4], M.S. Dixit[7], E. do Couto e Silva[12], J.E. Duboscq[8], E. Duchovni[26], G. Duckeck[8], I.P. Duerdoth[16], U.C. Dunwoody[5], P.A. Elcombe[5], P.G. Estabrooks[6], E. Etzion[23], H.G. Evans[9], F. Fabbri[2], B. Fabbro[21], M. Fanti[2], M. Fierro[2], M. Fincke-Keeler[28], H.M. Fischer[3], P. Fischer[3], R. Folman[26], D.G. Fong[17], M. Foucher[17], H. Fukui[24], A. Fürtjes[8], P. Gagnon[6], A. Gaidot[21], J.W. Gary[4], J. Gascon[18], N.I. Geddes[20], C. Geich-Gimbel[3], S.W. Gensler[9], F.X. Gentit[21], T. Geralis[20], G. Giacomelli[2], P. Giacomelli[4], R. Giacomelli[2], V. Gibson[5], W.R. Gibson[13], J.D. Gillies[20], J. Goldberg[22], D.M. Gingrich[30,a], M.J. Goodrick[5], W. Gorn[4], C. Grandi[2], P. Grannis[8], E. Gross[26], J. Hagemann[27], G.G. Hanson[12], M. Hansroul[8], C.K. Hargrove[7], J. Hart[8], P.A. Hart[9], M. Hauschild[8], C.M. Hawkes[8], E. Heflin[4], R.J. Hemingway[6], G. Herten[10], R.D. Heuer[8], J.C. Hill[5], S.J. Hillier[8], T. Hilse[10], D.A. Hinshaw[18], P.R. Hobson[25], D. Hochman[26], A. Höcker[3], R.J. Homer[1], A.K. Honma[28,a], R.E. Hughes-Jones[16], R. Humbert[10], P. Igo-Kemenes[11], H. Ihssen[11], D.C. Imrie[25], A. Jawahery[17], P.W. Jeffreys[20], H. Jeremie[18], M. Jimack[1], M. Jones[6], R.W.L. Jones[8], P. Jovanovic[1], C. Jui[4], D. Karlen[6], K. Kawagoe[24], T. Kawamoto[24], R.K. Keeler[28], R.G. Kellogg[17], B.W. Kennedy[20], B. King[8], J. King[13], S. Kluth[5], T. Kobayashi[24], M. Kobel[10], D.S. Koetke[8], T.P. Kokott[3], S. Komamiya[24], R. Kowalewski[8], R. Howard[29], P. Krieger[6], J. von Krogh[11], P. Kyberd[13], G.D. Lafferty[16], H. Lafoux[8], R. Lahmann[17], J. Lauber[8], J.G. Layter[4], P. Leblanc[18], P. Le Du[21], A.M. Lee[31], E. Lefebvre[18], M.H. Lehto[15], D. Lellouch[26], C. Leroy[18], J. Letts[4], L. Levinson[26], Z. Li[12], F. Liu[29], S.L. Lloyd[13], F.K. Loebinger[16], G.D. Long[17], B. Lorazo[18], M.J. Losty[7], X.C. Lou[8], J. Ludwig[10], A. Luig[10], M. Mannelli[8], S. Marcellini[2], C. Markus[3], A.J. Martin[13], J.P. Martin[18], T. Mashimo[24], P. Mättig[3], U. Maur[3], J. McKenna[29], T.J. McMahon[1], A.I. McNab[13], J.R. McNutt[25], F. Meijers[8], F.S. Merritt[9], H. Mes[7], A. Michelini[8], R.P. Middleton[20], G. Mikenberg[26], J. Mildenberger[6], D.J. Miller[15], R. Mir[26], W. Mohr[10], C. Moisan[18], A. Montanari[2], T. Mori[24], M. Morii[24], U. Müller[3], B. Nellen[3], B. Nijjhar[16], S.W. O'Neale[1], F.G. Oakham[7], F. Odorici[2], H.O. Ogren[12], C.J. Oram[28,a], M.J. Oreglia[9], S. Orito[24], J.P. Pansart[21], G.N. Patrick[20], M.J. Pearce[1], P. Pfister[10], P.D. Phillips[16], J.E. Pilcher[9], J. Pinfold[30], D. Pitman[28], D.E. Plane[8], P. Poffenberger[28], B. Poli[2], A. Posthaus[3], T.W. Pritchard[13], H. Przysiezniak[18], M.W. Redmond[8], D.L. Rees[8], D. Rigby[1], M. Rison[5], S.A. Robins[13], D. Robinson[5], J.M. Roney[28], E. Ros[8], S. Rossberg[10], A.M. Rossi[2], M. Rosvick[28], P. Routenburg[30], Y. Rozen[8], K. Runge[10], O. Runolfsson[8], D.R. Rust[12], M. Sasaki[24], C. Sbarra[2], A.D. Schaile[8], O. Schaile[10], F. Scharf[3], P. Scharff-Hansen[8], P. Schenk[4], B. Schmitt[3], H. von der Schmitt[11], M. Schröder[12], H.C. Schultz-Coulon[10], P. Schütz[3], M. Schulz[8], C. Schwick[27], J. Schwiening[3], W.G. Scott[20], M. Settles[12], T.G. Shears[5], B.C. Shen[4], C.H. Shepherd-Themistocleous[7], P. Sherwood[15], G.P. Siroli[2], A. Skillman[16], A. Skuja[17], A.M. Smith[8], T.J. Smith[28], G.A. Snow[17], R. Sobie[28], R.W. Springer[17], M. Sproston[20], A. Stahl[3], C. Stegmann[10], K. Stephens[16], J. Steuerer[28], B. Stockhausen[3], R. Ströhmer[11], D. Strom[19], P. Szymanski[20], H. Takeda[24], T. Takeshita[24], S. Tarem[26], M. Tecchio[9], P. Teixeira-Dias[11], N. Tesch[3], M.A. Thomson[15], S. Towers[6], T. Tsukamoto[24], M.F. Turner-Watson[8], D. Van den plas[18], R. Van Kooten[12], G. Vasseur[21], M. Vincter[28], A. Wagner[27], D.L. Wagner[9], C.P. Ward[5], D.R. Ward[5], J.J. Ward[15], P.M. Watkins[1], A.T. Watson[1], N.K. Watson[7],

P. Weber[6], P.S. Wells[8], N. Wermes[3], B. Wilkens[10], G.W. Wilson[4], J.A. Wilson[1], V-H. Winterer[10], T. Wlodek[26], G. Wolf[26], S. Wotton[11], T.R. Wyatt[16], A. Yeaman[13], G. Yekutieli[26], M. Yurko[18], W. Zeuner[8], G.T. Zorn[17].

[1]School of Physics and Space Research, University of Birmingham, Birmingham B15 2TT, UK
[2]Dipartimento di Fisica dell' Università di Bologna and INFN, I-40126 Bologna, Italy
[3]Physikalisches Institut, Universität Bonn, D-53115 Bonn, Germany
[4]Department of Physics, University of California, Riverside CA 92521, USA
[5]Cavendish Laboratory, Cambridge CB3 0HE, UK
[6]Carleton University, Department of Physics, Colonel By Drive, Ottawa, Ontario K1S 5B6, Canada
[7]Centre for Research in Particle Physics, Carleton University, Ottawa, Ontario K1S 5B6, Canada
[8]CERN, European Organisation for Particle Physics, CH-1211 Geneva 23, Switzerland
[9]Enrico Fermi Institute and Department of Physics, University of Chicago, Chicago IL 60637, USA
[10]Fakultät für Physik, Albert Ludwigs Universität, D-79104 Freiburg, Germany
[11]Physikalisches Institut, Universität Heidelberg, D-69120 Heidelberg, Germany
[12]Indiana University, Department of Physics, Swain Hall West 117, Bloomington IN 47405, USA
[13]Queen Mary and Westfield College, University of London, London E1 4NS, UK
[14]Birkbeck College, London WC1E 7HV, UK
[15]University College London, London WC1E 6BT, UK
[16]Department of Physics, Schuster Laboratory, The University, Manchester M13 9PL, UK
[17]Department of Physics, University of Maryland, College Park, MD 20742, USA
[18]Laboratoire de Physique Nucléaire, Université de Montréal, Montréal, Quebec H3C 3J7, Canada
[19]University of Oregon, Department of Physics, Eugene OR 97403, USA
[20]Rutherford Appleton Laboratory, Chilton, Didcot, Oxfordshire OX11 0QX, UK
[21]CEA, DAPNIA/SPP, CE-Saclay, F-91191 Gif-sur-Yvette, France
[22]Department of Physics, Technion-Israel Institute of Technology, Haifa 32000, Israel
[23]Department of Physics and Astronomy, Tel Aviv University, Tel Aviv 69978, Israel
[24]International Centre for Elementary Particle Physics and Department of Physics, University of Tokyo, Tokyo 113, and Kobe University, Kobe 657, Japan
[25]Brunel University, Uxbridge, Middlesex UB8 3PH, UK
[26]Particle Physics Department, Weizmann Institute of Science, Rehovot 76100, Israel
[27]Universität Hamburg/DESY, II Institut für Experimental Physik, Notkestrasse 85, D-22607 Hamburg, Germany
[28]University of Victoria, Department of Physics, P O Box 3055, Victoria BC V8W 3P6, Canada
[29]University of British Columbia, Department of Physics, Vancouver BC V6T 1Z1, Canada
[30]University of Alberta, Department of Physics, Edmonton AB T6G 2J1, Canada
[31]Duke University, Dept of Physics, Durham, NC 27708-0305, USA
[32]Technische Hochschule Aachen, III Physikalisches Institut, Sommerfeldstrasse 26-28, D-52056 Aachen, Germany

[a]Also at TRIUMF, Vancouver, Canada V6T 2A3

1 Introduction

Precise measurements of the τ lepton lifetime allow an important check of the assumption of lepton universality of the charged current electroweak interaction. One form of this check compares the lifetime, mass, and electronic branching ratio of the τ with the well-determined muon lifetime and mass:

$$\left(\frac{g_\tau}{g_\mu}\right)^2 = \left(\frac{\tau_\mu}{\tau_\tau}\right)\left(\frac{m_\mu}{m_\tau}\right)^5 \mathrm{BR}(\tau \to \mathrm{e}\overline{\nu}_\mathrm{e}\nu_\tau) \; . \tag{1}$$

The squared ratio of coupling constants in this relation undergoes a small modification (-0.04%) due to radiative corrections [1]. The electroweak couplings, g_μ and g_τ, are equal under the universality assumption. Over the last two years the results of this check have changed appreciably in both the central value and in the level of precision. First, new τ mass measurements [2, 3, 4] yielded values of the mass significantly lower than the previous world average [5]. In addition, the improved measurement precision of 0.0015% reduced the contribution of the τ mass uncertainty in the determination of the g_τ/g_μ ratio to a negligible level, relative to the less precisely measured τ lifetime and branching ratios. Although this improved the precision of the check, a possible deviation from unity which was previously observed persisted [6]. Second, new lifetime measurements were made [7, 8, 9, 10], which not only significantly decreased the contribution to the relative uncertainty from this source, but which were lower than the previous world average [5]. The new values indicated no discrepancy with universality.

We present an update of the OPAL τ lifetime measurement, based on the data recorded during 1992 and 1993, which is of significantly improved precision. The methods follow those of the previous measurement [9], which was based on the 1990 and 1991 data samples, and which may be referred to for more details. Two statistically independent techniques are used. The first is based on the impact parameter distribution of charged tracks from one-prong τ decays. The second is based on the decay length of vertices from three-prong τ decays. These measurements, and their combination, are discussed after introductory descriptions of the OPAL detector, the determination of the beam position and size, and the τ pair event selection and Monte Carlo.

2 The OPAL detector

OPAL is an experiment collecting data at the LEP $\mathrm{e^+e^-}$ storage ring, which operates at center-of-mass energies near the $\mathrm{Z^0}$ peak. Data taken during 1992 were at the single energy, $\sqrt{s} \simeq 91.16$ GeV. During 1993, half of the integrated luminosity was taken near the peak, with the remaining half equally divided between energy points approximately ± 1.8 GeV from the peak.

Since a complete description of the detector components can be found elsewhere [11, 12, 13], we describe briefly only those elements directly involved in this analysis. The coordinate

system is defined such that the z-axis follows the electron beam direction and the x-y plane is perpendicular to it, with the x-axis lying horizontally in the plane of the LEP ring. The polar angle θ is defined relative to the $+z$-axis, while the azimuthal angle ϕ is defined relative to the $+x$-axis. The radius, r, is the distance from the z-axis.

The central tracking system comprises z-chambers at the outer radius (just inside the solenoid), within which are contained the jet chamber, a vertex drift chamber, and a silicon strip vertex detector. Except for the silicon detector, the tracking chambers are contained in a 4 bar pressure vessel. The entire central tracking system is immersed in an axial magnetic field of 0.435 T. The large-volume jet chamber provides up to 159 radial measurements of the track from its first layer at 25.5 cm radius to the outermost at 183.5 cm. The average resolution achieved in the x-y plane is 130 μm. The vertex drift chamber provides 12 axial-layer measurements beginning at 10.3 cm radius from the beam axis and ending at 16.2 cm, together with 6 layers of stereo wires from radial positions of 18.8 cm to 21.3 cm. The typical spatial resolution achieved by the device is 50 μm for the first hit registered on a wire in a given event, and 90 μm for subsequent hits on the same wire.

A high precision silicon microvertex detector [12] surrounding the 5.3 cm-radius beryllium-composite beam pipe at the interaction point was commissioned during the 1991 run. This device provided two layers of silicon strip readout in the x-y plane, covering the angular region $|\cos\theta| \leq 0.8$. The layers were formed by concentric polygons of detector "ladders" whose centers were located at radii of 6.1 and 7.5 cm. Each ladder consisted of a detector array of 629 readout strips arranged parallel to the beamline. The inner layer had 11 such ladders, and the outer had 14. For 1993, that device was replaced with one providing additional hit information in the z-direction. The ladder arrangement of the new device [13] is identical to that of the previous one, with each ladder containing separate detectors providing z-information (readout strips perpendicular to the beam axis) and x-y information. The latter set of detectors are identical to those of the 1991/2 detector and only the information from these x-y ladders, common to both devices, was used in this analysis. Although the intrinsic detector resolution in x-y for both the 1991/2 and 1993 silicon detectors is about 5 μm [12], alignment uncertainties within OPAL limit the space-point resolution to about 9 μm. When combined with the surrounding drift chambers, the ensemble of tracking devices achieves an x-y impact parameter resolution of 16 μm in μ-pair and electron-pair events.

The τ production point is taken as the average beam spot position reconstructed from charged tracks collected from many consecutive events during a LEP fill [9]. Several beam position determinations are made over the course of a typical eight-hour fill of the machine. The beam position uncertainties are approximately $(21, 7)$ μm in (x, y).

A measurement of the horizontal size of the beam spot, σ_x, was made using the impact parameters of tracks with respect to the average beam spot position in collinear $Z^0 \to \mu^+\mu^-$ events. From these, we have determined $\sigma_x = 95 \pm 2$ μm averaged over the 1992 data, and 154 ± 2 μm averaged over the 1993 data. The LEP beam optics differed between the two years, giving rise to the significantly increased beam size in 1993. The vertical beam sizes were determined from multihadronic events to be 14 μm in 1992 and 16 μm in 1993. When taken together with variations of the size over the course of a fill, the overall uncertainties on the beam size are $(\delta\sigma_x, \delta\sigma_y) = (\pm 7, \pm 3)$ μm.

3 The τ-pair data and Monte Carlo samples

The OPAL detector recorded approximately 24 pb^{-1} integrated luminosity during 1992 and 34 pb^{-1} during 1993. Candidate τ-pair events were selected from these data by requiring two collimated, back-to-back, low multiplicity jets [14]. Events satisfying μ-pair, or electron-pair selection criteria were rejected. The angular acceptance for the selection was defined by $|\cos\theta_{\mathrm{thrust}}| \leq 0.9$, where θ_{thrust} is the polar angle of the event thrust axis. Monte Carlo studies indicate an efficiency of about 75% for selecting τ-pair events. The selection yielded a total of 28 792 events from the 1992 data, and 26 894 events from the 1993 data.

Additional reduction of backgrounds was performed for each analysis. Events contributing to the one-prong measurement had to have an angle of at least 2 mrad between the x-y projections of the summed momentum vectors of the charged particles in the hemispheres determined by the thrust axis. This reduced the sample size by 3.6% while reducing the backgrounds from μ-pair events by 36%. The residual background remaining in the one-prong data sample is $(1.51 \pm 0.51)\%$, of which most is from μ-pair events.

The background for the three-prong analysis comes from the tail of low multiplicity multihadron events passing the τ-pair maximum multiplicity cut of seven charged tracks. This component was reduced by two-thirds by rejecting events which also passed the OPAL multihadron selection [14], with a reduction of only 2.7% in the τ-pair data sample. The remaining multihadronic event background is $(0.25 \pm 0.25)\%$.

The KORALZ Monte Carlo program [15] was used for the simulation of $\mathrm{e^+e^-} \to \tau^+\tau^-$ events at $\sqrt{s} = 91.160$ GeV. Approximately 300 000 events were generated for each of two samples: one for the 1992 detector, using KORALZ version 3.8 [15]; and the other for the 1993 detector, using KORALZ version 4.0 [16]. The OPAL detector simulation [17] includes details of the material and geometry, and the efficiencies and responses of the detector elements. The simulated beam sizes were set to values corresponding to those of the particular year.

4 Lifetime measurement by impact parameter method

Decays of the τ lepton into a single charged track were used to perform a measurement of the τ lifetime by studying the distribution of miss distances of these tracks, with respect to the assumed τ production point as given by the beam position. Candidate one-prong τ decay tracks were selected by requiring exactly one charged track in an event hemisphere, as determined by the thrust axis. Both hemispheres of each event were allowed in the selection. The impact parameter, d_0, of a track in the x-y plane was given a positive sign if the track crossed the thrust axis in the same hemisphere, relative to the beam position, in which it lay and was signed negative otherwise. Note that at center-of-mass energies near the Z^0 peak the impact parameter is independent of the τ boost, and is thus invariant with respect to the slight changes in the center-of-mass energy for the different energy scan points of the 1993 data.

The d_0 distributions of the one-prong τ decay candidates selected from the data were compared with the Monte Carlo distributions obtained using an input lifetime of 303.5 fs. We

used the 10% trimmed means, i.e., the means of the distributions remaining after the lowest and highest 5% of entries were removed, for the comparison. It has been verified with Monte Carlo studies that the 10% trimmed mean scales linearly with the input lifetime, and produces a trimmed mean that is consistent with zero when the input tau lifetime is set to zero. The formula for the statistical error on the trimmed mean has been given previously [9, 18].

The tracks used for this analysis were required to have at least one silicon hit, to have at least half the maximum possible number of hits in the central jet chamber, a total track impact parameter uncertainty (including the beam size) of less than 0.1 cm, and a χ^2 per degree of freedom from the track reconstruction of less than 10. A total of 35 168 tracks from the 1992 data and 32 703 tracks from the 1993 data were selected. The tracking resolutions of the τ Monte Carlo were adjusted to match those of the data using independent samples of μ-pair Monte Carlo and data. These comparisons were used to determine extra Gaussian smearing factors that were then applied to the Monte Carlo samples for the 1992 or 1993 data. The extra smearing required was about 20 μm, which was applied in quadrature to the d_0 resolution from tracking only, which averaged 35 μm. These effects are, however, much smaller than the smearing which is caused by the large horizontal beam size.

The high eccentricity of the beam ellipse causes the widths of the impact parameter distributions for horizontally-lying tracks to be much narrower than those of vertical tracks. A single trimmed mean cut for all tracks would therefore tend to select against vertical tracks, and would be less effective in eliminating tracks in the tails of the distribution of horizontally-lying tracks. We therefore divided the d_0 distributions of data and Monte Carlo samples into six equally-sized regions in ϕ, according to the effective beam width presented to the track. The lifetimes in these bins are shown for both the 1992 and 1993 data samples in Figure 1. These measurements are combined for the final result. The weighted average lifetimes before background corrections were 285.8 ± 4.4 fs for the 1992 data sample, and 283.7 ± 5.3 fs for the 1993 data, where only the statistical errors of the data are given. The 1993 data have less statistical weight due primarily to the larger beam size for that year.

The impact parameter distribution for the combination of 1992 and 1993 tracks, together with the Monte Carlo prediction, is shown in Figure 2. This figure is for illustrative purposes only, since the lifetime measurement is based on the 12 divisions of this distribution, into ϕ bins and according to year.

Several checks of the results have been made. The τ selection cuts were found to cause no bias in the measurement. Although the thrust axis obtained from charged tracks alone was used to sign the impact parameters, event axes which include electromagnetic calorimeter information give statistically compatible results. In addition, results obtained from divisions of the data according to other variables such as the event visible energy, $\cos\theta_{\rm thrust}$, and number of tracks in the opposite hemisphere, are consistent.

The systematic error is composed of contributions due to detector resolution effects, uncertainties in the Monte Carlo physics inputs, backgrounds, and the limited sample sizes of the Monte Carlo data sets. The detector resolution effects in turn consist of the uncertainty in providing the correct smearing prescription for the Monte Carlo, residual detector calibration and alignment uncertainties, the beam size uncertainty, and the beam position uncertainty. The limit of residual detector alignment uncertainties was obtained from a study of the impact

parameter distributions in μ-pair events selected from the data. The beam position and size contributions were determined from the ranges of uncertainty in these parameters discussed above. The uncertainties in physics inputs are due primarily to the generator decay mode branching fraction uncertainties, since different decay modes lead to slightly different trimmed means. The systematic error contributions for these effects were determined from the Monte Carlo by varying the given parameter within its range of uncertainty, and determining the resulting change for the Monte Carlo sample trimmed mean. The correction to the lifetime for the residual background of electron-pair, μ-pair, two-photon, and multihadron tracks remaining in the one-prong sample was determined from Monte Carlo studies to be $(+0.82 \pm 0.28)\%$.

The full résumé of systematic errors for the one-prong lifetime analysis is given in Table 1. The contributions due to background and Monte Carlo branching ratio uncertainties are determined once for both years of data and are therefore correlated in the combined lifetime. In addition, correlations may exist between the systematic error contributions for detector calibration and alignment since the same methods are used in determining the alignment constants for both years. Allowing for full correlations among these three items we find the combined one-prong lifetime:

$$\tau_1 \;=\; 287.2 \;\pm\; 3.4\,(\text{stat}) \;\pm\; 2.0\,(\text{sys})\ \text{fs}\ . \tag{2}$$

source	1992	1993
resolution matching of MC	0.56%	0.35%
detector calibration & alignment	0.14%	0.12%
beam size uncertainties	0.40%	0.36%
beam position uncertainties	0.15%	0.09%
background fractions	0.28%	
MC decay mode branching ratios	0.18%	
MC statistics	0.50%	0.59%
total systematic error	0.94%	0.86%

Table 1: Systematic error contributions for the one-prong lifetime measurements. For the Monte Carlo (MC) decay mode branching ratio and background uncertainties, a single determination was made for both years.

5 Lifetime measurement by decay length method

Decays of the τ lepton into three charged tracks provide an opportunity to measure directly the decay lengths of τ particles. A maximum likelihood fit is used to extract the average τ decay length, which is converted directly into a lifetime measurement by using the known mass and boost velocity of the parent τ lepton. Three-prong τ decay candidates were selected from thrust hemispheres which contained exactly three tracks of total charge ± 1, after the elimination of tracks from probable photon conversions and K^0_S decays [9]. Each track was required to have a χ^2 per degree of freedom, from the track reconstruction, of less than 10. All such three-track combinations were subjected to a vertex fit, and those having a probability from this fit of less than 0.01 were rejected. The same basic vertex quality selection was applied as in the previous analysis [9], which required that at least two of the three tracks contain either silicon detector

hits, or else a majority of first hits in the vertex drift chamber. The efficiency for this selection was approximately 91%.

The reconstructed beam position and error ellipse were combined with the fitted three-prong vertex position and error ellipse, and with the event thrust axis direction constraint, in a least-squares fit for the most probable decay length and error in the x-y plane [9]. The polar angle of the thrust axis was used to obtain the three-dimensional decay length and error used in the maximum likelihood fit for the most probable average decay length.

In our previous analysis [9] the maximum likelihood fit determined the average decay length, and a scale factor for the errors which allowed for any systematic error in our description of the detector resolution function. For the present analysis, the fit was modified by the addition of two more parameters — a second scale factor for the decay length errors and a fraction of the total set of errors corresponding to this scale factor. The extra factors allows the fit to accommodate better both the majority of measurements whose errors are determined accurately, and the small component of vertices whose errors may be significantly underestimated. The change in the resulting lifetime is negligible, however, when reverting to the single error scale factor mechanism. The fit performed with the second scale factor had a primary resolution scale factor consistent with one (1.019 ± 0.038 in the 1992 data, and 0.976 ± 0.031 in the 1993 data), with a two-three percent of events described by a second scaling factor of approximately three. The use of a single scale factor fit yielded a value of approximately 1.1.

The maximum likelihood fit was applied only to those decay candidates having three-dimensional decay length errors less than 0.6 cm, and lying within the decay length range $[-0.8, +1.5]$ cm (a renormalization procedure accounts for the reduced range in the fit [9], ensuring that no bias is introduced). The total numbers of three-prong decay length measurements entering into the fit were 4671 from the 1992 data, and 4417 from the 1993 data. The average decay length was converted to a lifetime with a Lorentz factor, calculated at the various center-of-mass energies, which includes corrections for the effects of initial state radiation. This Lorentz factor assumed a τ mass of 1777.0 MeV/c^2. The lifetimes, before background correction, were 284.5 ± 4.8 fs from the 1992 data, and 292.6 ± 5.3 fs from the 1993 data. The decay length distribution for the combination of both data samples is shown in Figure 3, together with a curve representing the result of a maximum likelihood fit. Again, this figure is for illustrative purposes only since the lifetimes are fitted separately for the two years when determining the overall result.

Results obtained from various divisions of the data by polar angle, azimuth (shown in Figure 4), and visible energy are consistent. Variations of the endpoints of the decay length window cut, or of the decay length error cut produced consistent results, as did variants of the event axis which included electromagnetic calorimetry or even replacement by the three-prong momentum.

Systematic error contributions arise from detector calibration uncertainties, thrust direction uncertainties, beam position and size uncertainties, potential biases remaining in the analysis method, and initial state radiation corrections. Detector calibration uncertainties for the silicon microvertex detector were estimated by allowing for coherent radial motions in the ladder positions of up to ± 50 μm, which was estimated to be an upper limit for remnant radial shifts as determined from studies of track residuals across the width of individual ladders. Uncertainties

from the vertex drift chamber were estimated from the residual 0.05% uncertainty in the gas drift velocity. The latter effect is much reduced by the presence of silicon hits on most of the tracks. Both azimuthal ($\sim$ 1 mrad) and polar angle ($\sim$ 1 mrad) thrust axis uncertainties are included. The systematic error contributions from the beam position and size uncertainties mentioned above are small. Tests made with the Monte Carlo samples proved that the fitted lifetime is consistent with the input. However, the limited statistics lead to an uncertainty on this check of 0.57% in each of the two years, which is included as a systematic error effect representing our estimation of the limit of residual biases remaining in the method.

The full list of systematic errors for each of the two data samples is given in Table 2. In forming the combination, we allowed for correlations between the systematic error contributions due to detector alignment and calibration, since the same methods of determining these were used in both years; between the thrust axis bias terms, since these likewise result from residual miscalibrations of the detector; and for the multihadronic background correction factor of $(+0.25 \pm 0.25)\%$, which was determined once for the entire data sample. The lifetime obtained after applying the background correction factor is

$$\tau_3 \;=\; 288.9 \;\pm\; 3.6\;(\mathrm{stat}) \;\pm\; 1.7\;(\mathrm{sys})\;\mathrm{fs}\;. \tag{3}$$

source	1992	1993
silicon detector alignment	0.40%	0.40%
vertex drift chamber calibrations	0.03%	0.03%
thrust ϕ biases	0.013%	0.011%
thrust θ biases	0.06%	0.06%
beam position uncertainties	0.070%	0.041%
beam size uncertainties	0.120%	0.093%
bias limits (Monte Carlo statistics)	0.57%	0.57%
multihadronic background	0.25%	
total systematic error	0.76%	0.75%

Table 2: Systematic error contributions for the three-prong lifetime measurements.

We have repeated the decay length analysis of the three prong decays using a slightly different selection and vertex fitting method, in order to investigate the sensitivity of the measurement to the silicon detector resolution and its calibration with respect to the drift tracking chambers. For this analysis, at least one silicon detector hit was required on each of the three tracks. The vertex was determined from a fitting procedure which allowed the silicon hits to be weighted differently, with respect to the matching track segments extrapolated from the drift chambers, than in the standard OPAL track fits. The drift chamber tracks and the silicon hits were combined in a simultaneous best fit for the vertex position and the final track parameters. This feature of the analysis facilitates checking for the effects of hit mis-assignments which may occur in the dense track environment of three-prong τ decays. No effects of this nature were found.

The remainder of the analysis is the same as that described above. The maximum likelihood fit, applied to the 6030 vertices from the 1992 and 1993 data which had decay lengths less than

2.5 cm and errors less than 0.3 cm, produced the result:

$$\tau_3 \;=\; 289.0 \;\pm\; 4.0\;(\mathrm{stat}) \;\pm\; 2.7\;(\mathrm{sys})\;\mathrm{fs}\;.$$

This result is in good agreement with the analysis presented above. The stricter selection criterion requiring silicon hits on all three tracks reduces the statistics for this measurement due to the reduced $|\cos\theta|$ acceptance, although the events selected are those having the best measurement resolution. The measurement also has different sensitivities in certain systematic error contributions, being especially more sensitive to silicon detector alignment uncertainties and the relative weighting (resolution) assumed for the silicon hits with respect to the drift chamber. It is presented here as an independent confirmation of the previous result.

6 Summary

The one-prong and three-prong results are combined to give the OPAL result for the τ lifetime as measured with the 1992 and 1993 data samples. The two measurements are statistically independent, since they were obtained from different sets of τ decays. We find the result from the OPAL data presented here to be:

$$\tau_\tau(1992+1993) \;=\; 288.1 \;\pm\; 2.5\;(\mathrm{stat}) \;\pm\; 1.3\;(\mathrm{sys})\;\mathrm{fs}. \qquad (4)$$

This value is in good agreement with the published OPAL result [9] of $291.9 \pm 5.1 \pm 3.1$ fs, found in the previous analysis of the 1990 and 1991 data. The results are combined, allowing for correlations between systematic error contributions for the background estimates of the one-prong analyses, and for the detector calibrations, thrust axis biases, and radiative corrections terms in the three-prong analyses. We find:

$$\tau_\tau \;=\; 288.8 \;\pm\; 2.2\;(\mathrm{stat}) \;\pm\; 1.4\;(\mathrm{sys})\;\mathrm{fs}. \qquad (5)$$

Our measured value is consistent with previously-published values [7, 8, 10], and represents the most precise determination of the τ lifetime to date.

The combined lifetime measurement can be used, together with world-average values of the τ leptonic branching ratios [5], to repeat the charged-current lepton universality test. We combine the electronic and muonic τ branching ratios (thereby assuming e-μ universality, which is confirmed to better than the 0.2% level [19, 20]) to find $\overline{\mathrm{BR}}(\tau \to \mathrm{e}\overline{\nu}_\mathrm{e}\nu_\tau) = (17.88 \pm 0.20)\%$. The measured ratio of coupling constants from Equation 1 gives:

$$\left(\frac{g_\tau}{g_\mu}\right) \;=\; 1.005 \;\pm\; 0.007\;, \qquad (6)$$

in agreement with the hypothesis of τ-μ lepton universality.

Acknowledgements

It is a pleasure to thank the SL Division for the efficient operation of the LEP accelerator, the precise information on the absolute energy, and their continuing close cooperation with our

experimental group. In addition to the support staff at our own institutions we are pleased to acknowledge the
Department of Energy, USA,
National Science Foundation, USA,
Particle Physics and Astronomy Research Council, UK,
Natural Sciences and Engineering Research Council, Canada,
Fussefeld Foundation,
Israel Ministry of Science,
Israel Science Foundation, administered by the Israel Academy of Science and Humanities,
Minerva Gesellschaft,
Japanese Ministry of Education, Science and Culture (the Monbusho) and a grant under the Monbusho International Science Research Program,
German Israeli Bi-national Science Foundation (GIF),
Direction des Sciences de la Matière du Commissariat à l'Energie Atomique, France,
Bundesministerium für Forschung und Technologie, Germany,
National Research Council of Canada,
A.P. Sloan Foundation and Junta Nacional de Investigação Científica e Tecnológica, Portugal.

References

[1] W. J. Marciano and A. Sirlin, Phys. Rev. Lett. **61** (1988) 1815.

[2] BES Collaboration, J.Z. Bai et al., Phys. Rev. Lett. **69** (1992) 3021.

[3] ARGUS Collaboration, H. Albrecht et al., Phys. Lett. **B292** (1992) 221.

[4] CLEO Collaboration, R. Balest et al., Phys. Rev. **D47** (1993) 3671.

[5] Particle Data Group, K. Hikasa et al., Phys. Rev. **D45** (1992) 1.

[6] W.J. Marciano, Phys.Rev. **D45** (1992) 721.

[7] CLEO Collaboration, M. Battle et al., Phys. Lett. **B291** (1992) 488.

[8] ALEPH Collaboration, D. Buskulic et al., Phys. Lett. **B297** (1992) 432.

[9] OPAL Collaboration, P. D. Acton et al., Z. Phys. **C59** (1993) 183.

[10] DELPHI Collaboration, P. Abreu et al., Phys. Lett. **B302** (1993) 356.

[11] OPAL Collaboration, K.Ahmet et al., Nucl. Instrum. and Meth. **A305** (1991) 275.

[12] P.P. Allport et al., Nucl. Instrum. and Meth. **A324** (1993) 34.

[13] P.P. Allport et al., *The OPAL Silicon Strip Microvertex Detector with Two Coordinate Readout*, CERN-PPE/94-16 (1994), submitted to Nucl. Instrum. and Meth.

[14] OPAL Collaboration, G. Alexander et al., Z. Phys. **C52** (1991) 175.

[15] S. Jadach, B.F.L. Ward, and Z. Was, Comput. Phys. Commun. **66** (1991) 276.

[16] S. Jadach, B.F.L. Ward, and Z. Was, Comput. Phys. Commun. **79** (1994) 503.

[17] J. Allison et al., Nucl. Instrum. and Meth. **A317** (1992) 47.

[18] A. C. Janissen, *Measurement of the Tau Lepton Lifetime at OPAL* (Ph.D. Thesis), Ottawa-Carleton Institute for Physics (1993).

[19] D. Britton, et al., Phys. Rev. Lett. **68** (1992) 3000.

[20] G. Czapek, et al., Phys. Rev. Lett. **70** (1993) 17.

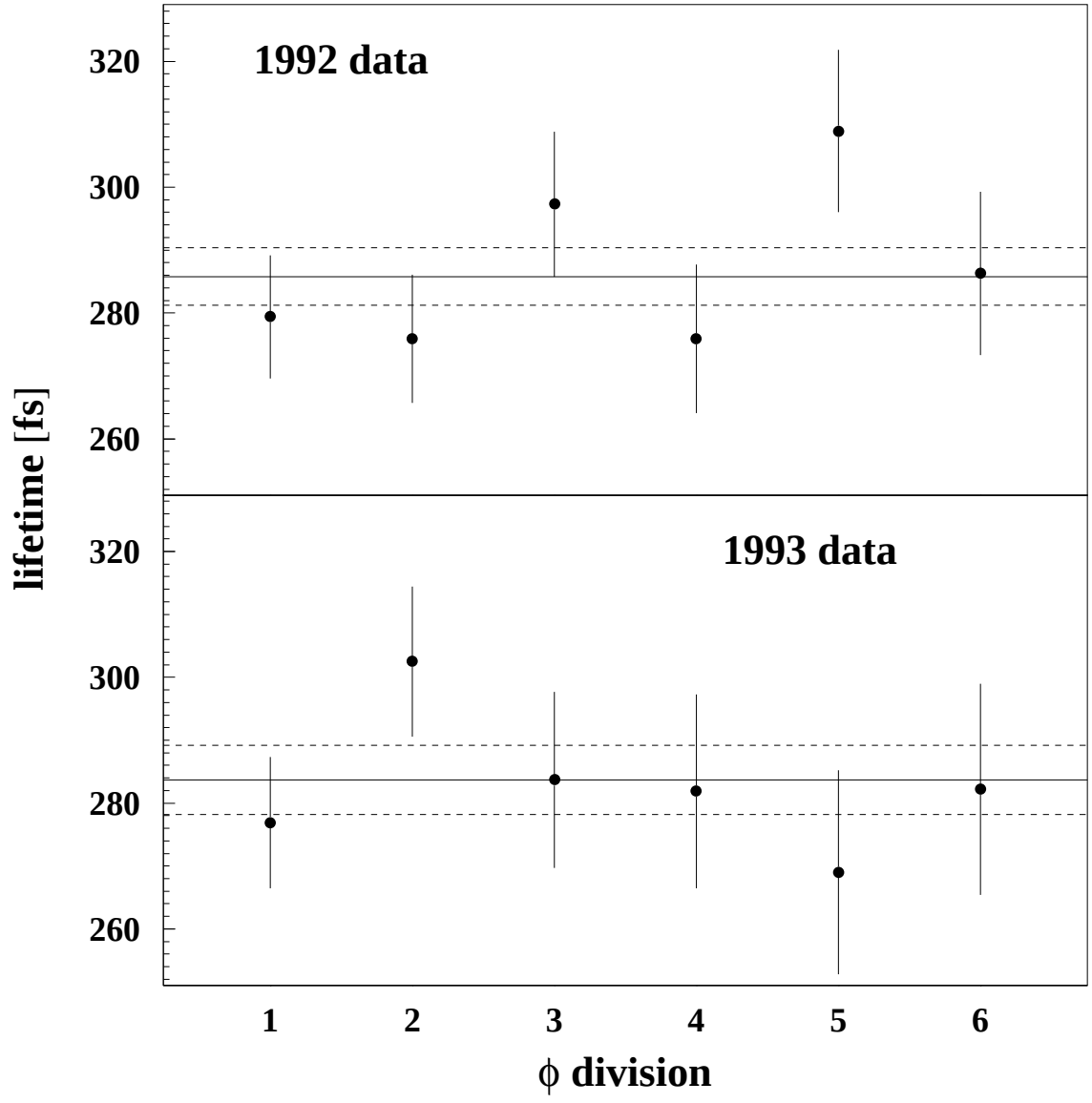

Figure 1: The lifetimes, uncorrected for backgrounds, measured in the ϕ divisions discussed in the text, for the impact parameter analyses of the 1992 and 1993 data. Division 1 is the set of tracks within 15° of horizontal, while division 6 is the set within 15° of vertical. The other divisions are equally-sized ranges in azimuth, according to the amount of the horizontal beam size which is intercepted. The solid and dotted lines for each year give the weighted average and uncertainty when the results from all six bins are combined.

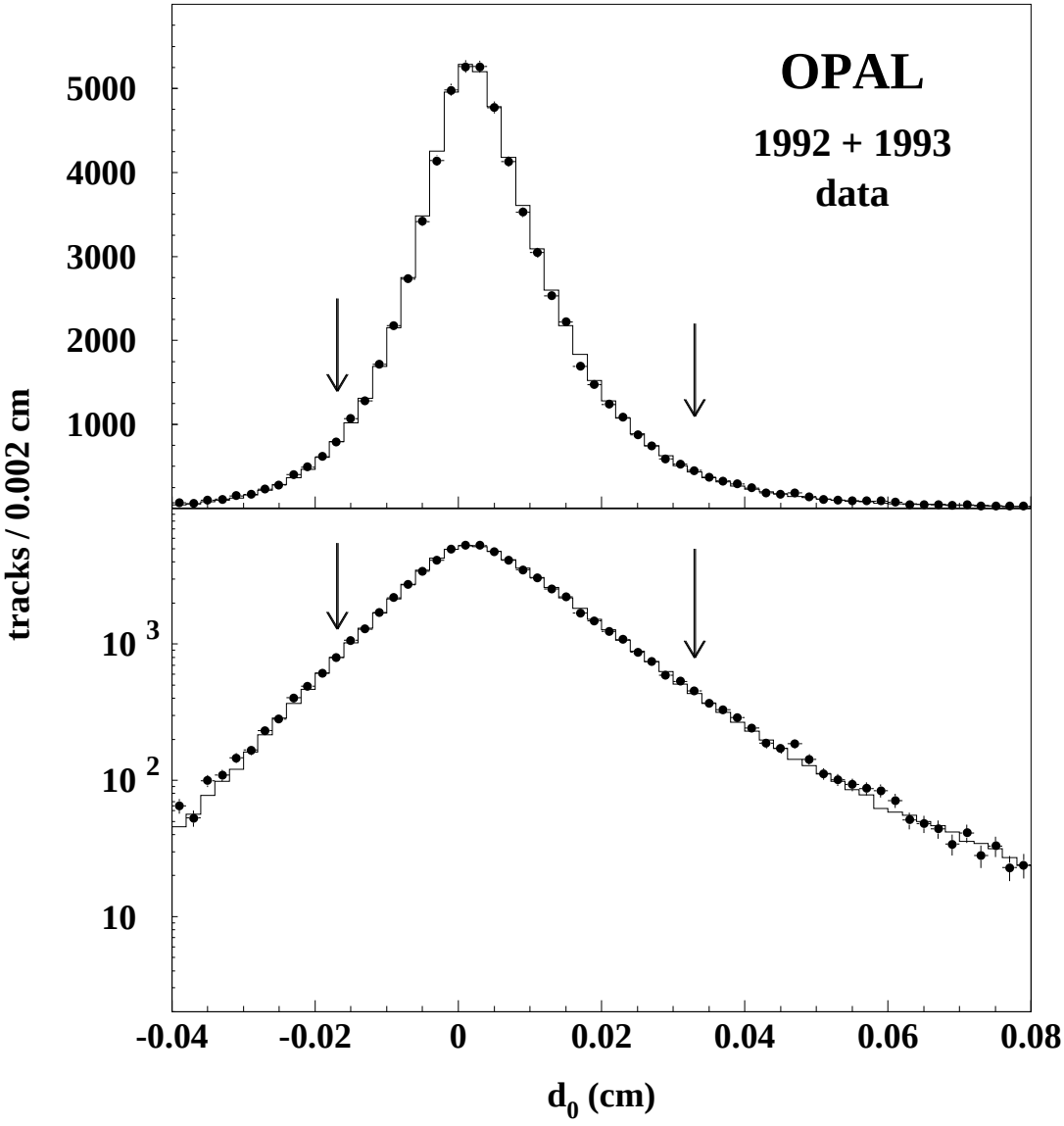

Figure 2: The impact parameter distribution for the combined 1992 and 1993 data samples (points), together with the combined prediction from the Monte Carlo sets of the two years when reweighted for lifetimes equal to the measured values (histogram). The arrows indicate the limits of the 10% trimmed mean of the distribution. This figure is for illustration only; the measurements of the lifetime are performed separately for each year and by divisions into six equally-sized azimuthal bins within each year (see Figure 1), and then combined in a weighted average. A "χ^2" calculated over the interval $[-0.02, +0.04]$ cm, which just encloses the trim range, gives 32.6 for the 30 bins in this region.

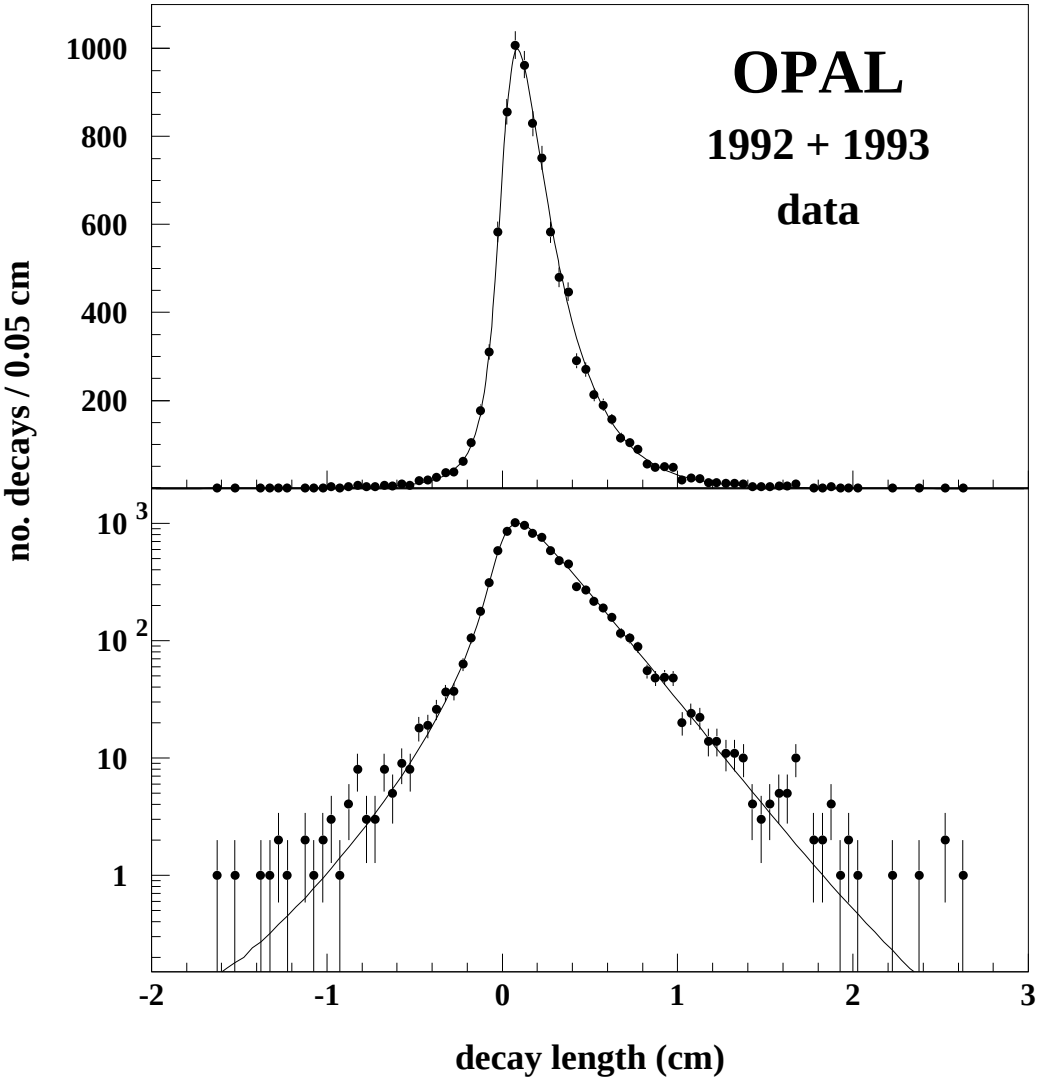

Figure 3: The distribution of three-prong decay lengths which have decay length error less than 0.6 cm, together with a curve representing the result of the maximum likelihood fit to the set of decay lengths lying within the window $[-0.8, +1.5]$ cm. This figure is for illustration only; the measurements of the lifetime are performed separately for each of the 1992 and 1993 years and then combined for the result. A "χ^2" calculated over the window range of the fit gives 25.5 for the 41 bins in this region.

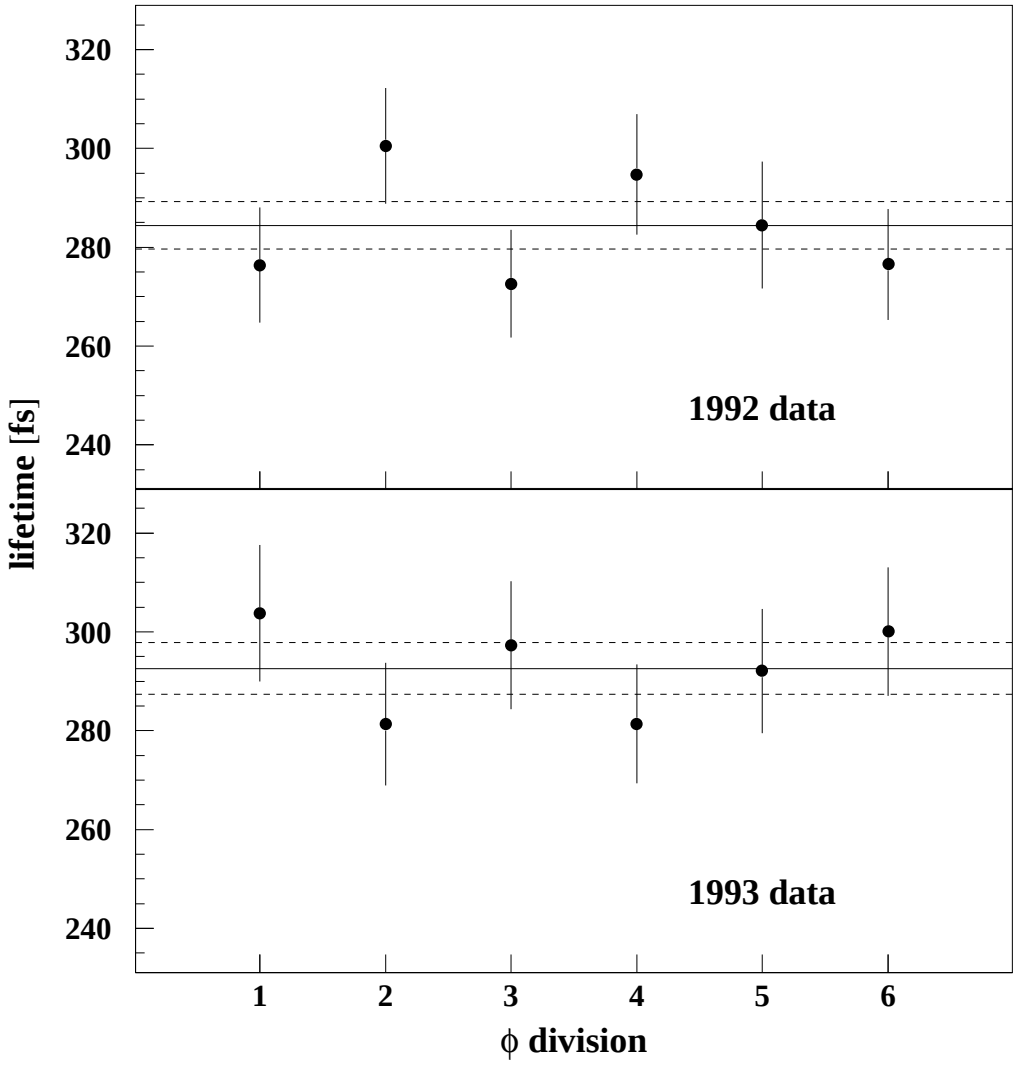

Figure 4: The lifetimes obtained from division of the three-prong decay length distributions into six equally-sized bins in azimuth, with the first bin beginning at zero.